SLAC-TN-69-6
R. Fowkes
July 1969

EFFECT OF IMPERFECT MATCHING AND PHASING IN SUPERCONDUCTING ACCELERATOR FEEDBACK LOOP WITH BEAM LOADING

Part I—Matching Considerations

Introduction

The use of external feedback in a superconducting accelerator has been studied in considerable detail by Neal[1] and others. By recirculating the rf power back through the input end of the accelerator the conversion efficiency of the accelerator can be made close to 100%. An alternative to the external feedback loop is internal feedback in the form of a standing wave accelerator. The beam conversion efficiency is nearly as high, but it suffers from a higher ratio of peak to average electric fields in the accelerating section. We can resolve the standing wave field configuration into its forward and backward wave components. The backward wave experiences no net exchange with the electron beam. Therefore, half of the stored energy is not being used, but is still contributing to i^2R losses in the accelerator walls and increasing the cost of refrigeration. For a given beam energy, the electric field strength at each maxima in a π mode standing wave structure is about 31% higher than for the same energy in the $2\pi/3$ mode traveling-wave structure with feedback. Hence a strong case is made for the TW structure with feedback.

There are some difficulties, however, with the TW accelerator with feedback which are not present to nearly the extent in the standing-wave accelerator. Some of these problems will be discussed in detail in this paper. The first problem discussed is the effect of a small perturbation or reflection in the waveguide loop. Also, the effect of an imperfectly matched dummy load will be covered. Then, the effect of a small error in the electrical length of the loop and in the phase of the bunched electron beam will be discussed. Lastly, the combined effects of these perturbations will be discussed.

Ideal Superconducting Accelerator with Feedback Under Steady State Conditions

A schematic of a traveling-wave accelerator and feedback loop is shown in Fig. 1. The bridge is assumed to be an ideal lossless directional coupler with

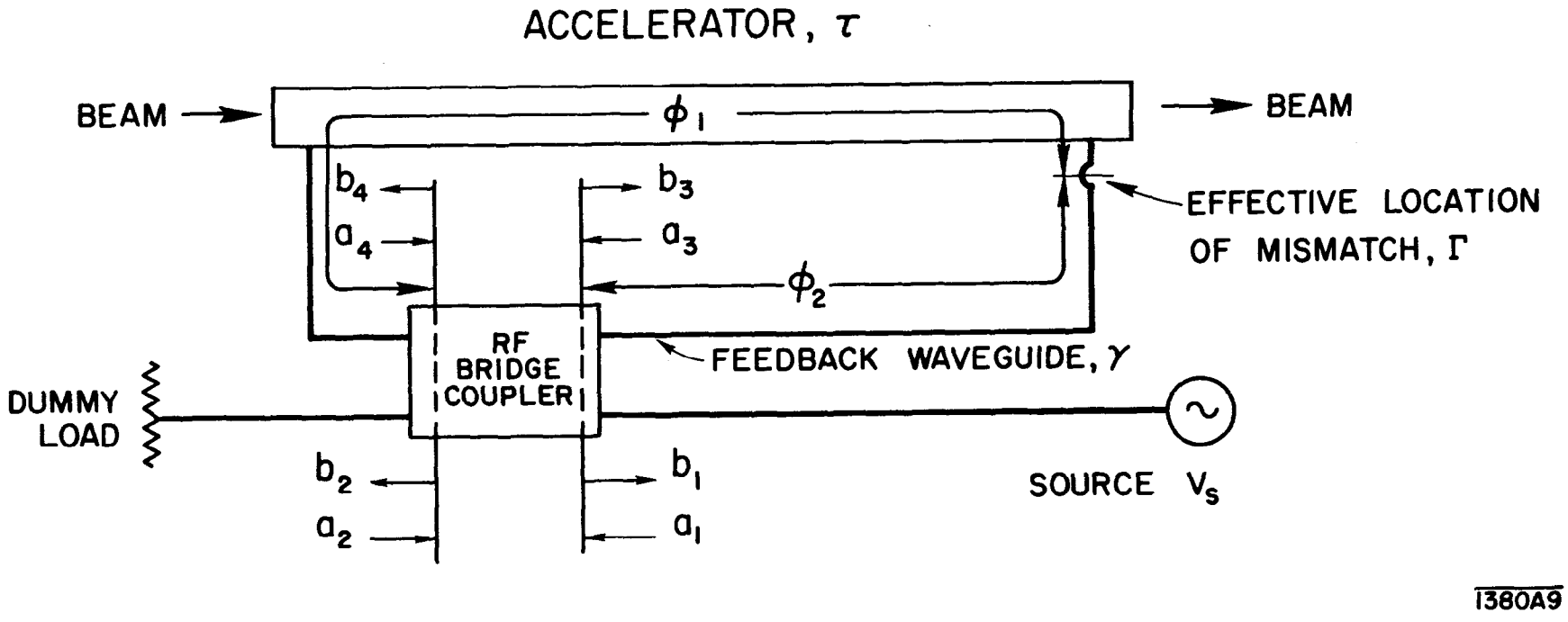

Fig. 1

Accelerator and feedback loop schematic. Bridge coupler reference planes are chosen so there is zero phase shift for straight ahead waves and 90 degrees for coupled waves.

a coupling ratio given in db by

$$C = 10 \log_{10} (1+g). \tag{1}$$

The tentative value for g at 2856 MHz is 5460.

Consider a voltage wave V_s incident upon arm 1 of the bridge coupler. A very small fraction of this wave initially is coupled into the accelerator and feedback loop while the rest goes into the dummy load connected to arm 2 of the bridge coupler. The wave coupled from arm 1 to arm 4 of the bridge into the loop before buildup has begun to occur is

$$\frac{jV_s}{(1+g)^{1/2}}$$

where $j = \sqrt{-1}$ and takes into account that the coupled wave has shifted 90^o with respect to the wave V_s. A transient analysis of the accelerating wave buildup was shown by Neal[1] for the ideal case where the loop is perfectly reflectionless and the phase length around the loop is an exact multiple of 2π.

It is necessary to use a scattering matrix approach, however, to develop exact expressions for the steady-state behavior of the accelerating wave for the non-ideal case where there are small reflections within the loop. In order to become familiar with this type of notation we can first develop the steady-state expression for the accelerating wave for the ideal case.

We can begin by labeling the four arms of the input bridge as shown in Fig. 1. Incoming waves will be represented by a_m and scattered waves by b_n. These are related to each other by the scattering coefficients where

$$b_n = S_{mn} a_m \tag{2}$$

Using scattering matrix notation

$$\begin{vmatrix} b_1 \\ b_2 \\ b_3 \\ b_4 \end{vmatrix} = \begin{vmatrix} S_{11} & S_{12} & S_{13} & S_{14} \\ S_{21} & S_{22} & S_{23} & S_{24} \\ S_{31} & S_{32} & S_{33} & S_{34} \\ S_{41} & S_{42} & S_{43} & S_{44} \end{vmatrix} \times \begin{vmatrix} a_1 \\ a_2 \\ a_3 \\ a_4 \end{vmatrix} . \tag{3}$$

Symmetry requires that

$$S_{12} = S_{34} \text{ and } S_{14} = S_{23} . \tag{4}$$

Reciprocity requires that

$$S_{14} = S_{41} = S_{23} = S_{32} . \tag{5}$$

Since the bridge is assumed to be an ideal directional coupler

$$S_{11} = S_{22} = S_{33} = S_{44} = 0. \tag{6}$$

From Eq. (1)

$$S_{14} = S_{41} = S_{32} = S_{23} = j\left(\frac{1}{1+g}\right)^{1/2} \tag{7}$$

Since the coupler is lossless

$$S_{12} = S_{21} = S_{34} = S_{43} = \left(\frac{g}{1+g}\right)^{1/2} \tag{8}$$

For large coupling ratios $S_{14} \ll 1$ and $g \gg 1$.

We can now write the equations for the accelerator/waveguide loop in terms of incident and scattered waves at the four arms of the bridge coupler.

$$b_1 = 0 \cdot a_1 + \left(\frac{g}{1+g}\right)^{1/2} a_2 + 0 \cdot a_3 + j\left(\frac{1}{1+g}\right)^{1/2} a_4 \tag{9}$$

$$b_2 = \left(\frac{g}{1+g}\right)^{1/2} a_1 + 0 \cdot a_2 + j\left(\frac{1}{1+g}\right)^{1/2} a_3 + 0 \cdot a_4 \tag{10}$$

$$b_3 = 0 \cdot a_1 + j\left(\frac{1}{1+g}\right)^{1/2} a_2 + 0 \cdot a_3 + \left(\frac{g}{1+g}\right)^{1/2} a_4 \tag{11}$$

$$b_4 = j\left(\frac{1}{1+g}\right)^{1/2} a_1 + 0 \cdot a_2 + \left(\frac{g}{1+g}\right)^{1/2} a_3 + 0 \cdot a_4 \tag{12}$$

The incident wave equations on the low power (arms 1 and 2) side of the bridge for a reflectionless dummy load are

$$a_1 = V_s \tag{13}$$

$$a_2 = 0 \tag{14}$$

The equation for a_4 on the high power side of the coupler (arms 3 and 4) contains both a passive and an active term. The passive term is merely the voltage transmission coefficient for the accelerator and feedback waveguide. The active term takes into account the energy that is transferred to the electron beam. This is most easily handled by the superposition of the voltage wave induced by the electron beam along with the wave from the rf source. Hence the last two equations are

$$a_3 = b_4 e^{-(\tau + \gamma + j\phi)} - jV_s e^{-(\gamma + j\psi)} \frac{1 - e^{-\tau}}{(2\tau)^{1/2}} i_n \tag{15}$$

$$a_4 = 0 \tag{16}$$

where

γ = attenuation parameter of feedback portion of waveguide in nepers

τ = altenuation parameter of accelerator portion of loop in nepers

V_s = voltage wave into arm 1 from source

V_b = voltage wave induced by the electron beam

ϕ = phase length around accelerator/waveguide loop

i_n = normalized electron beam current (see Eq. (18))

ψ = phase angle between the bunched electron beam and the impressed voltage wave $jV_s/(1+g)^{1/2}$ from the source.

The initial voltage wave coming out of the accelerator that is induced by the bunched electron beam is given by[1]

$$\frac{V_b}{V_s} = -je^{-j\psi} \frac{(1-e^{-\tau})}{(2\tau)^{1/2}} i_n \tag{17}$$

The normalized electron-beam current, i_n is defined by[1]

$$i_n \equiv \left(\frac{i^2 r_0 \ell}{P_s} \right)^{1/2} \tag{18}$$

where

i = peak electron beam current

r_0 = accelerator shunt impedance per unit length

ℓ = accelerator length

P_s = power from source into arm 1 of bridge.

The negative sign in Eq. (17) indicates that when the electron bunches are in phase with the impressed rf wave $[jV_s/(1+g)^{1/2}]$ before buildup, the induced wave is 180 degrees out of phase with the impressed rf wave. The "j" appears since V_b is normalized to V_s, taking into account the 90 degree phase shift in the bridge coupler. Solving Eqs. (9) through (12) we obtain

$$\frac{V_0}{V_s} = \frac{b_4}{a_1} = j \frac{1 - g^{1/2} e^{-(\gamma + j\psi)} \frac{(1-e^{-\tau})}{(2\tau)^{1/2}} i_n}{(1+g)^{1/2} - g^{1/2} e^{-(\tau + \gamma + j\phi)}} \tag{19}$$

which is the steady-state normalized accelerating voltage wave. This is expressed in complex form. For $\phi = n2\pi$ where n is an integer and $\psi = 0$ (i.e., beam is in

phase with the accelerating wave) Eq. (19) is identical to that obtained in Ref. 1. It should be mentioned at this point that the maximum rf power is transferred to the electron beam when $i_n \approx (2g\tau)^{-1/2}$.[1] This will henceforth be referred to as the design current. Equation (19) reduces approximately to $g^{1/2}$ at the design current.

Non-Ideal Superconducting Accelerator with Mismatch in Feedback Loop Under Steady-State Condition

Extreme care will be taken in the machining and matching of the accelerator structure and waveguide feedback loop. It will be impossible, however, to eliminate reflections entirely and these residual reflections must be tuned out to several orders of magnitude better than normally required for efficient rf power transmission. The effect of any residual reflections on the steady-state accelerating wave will be examined here. Waves scattered in the backward direction will build up just as the desired wave launched through the bridge coupler builds up in the forward direction. A transient analysis for multiple discreet mismatches becomes highly complex and will not be treated in this paper.

A number of very small mismatches in the resonant loop can be represented by a single mismatch discreetly located and having the scattering matrix

$$S_\Gamma = \begin{vmatrix} j\Gamma & (1-\Gamma^2)^{1/2} \\ (1-\Gamma^2)^{1/2} & j\Gamma \end{vmatrix} \qquad (20)$$

where Γ is the magnitude of the effective reflection coefficient in the waveguide part of the loop. If Γ is to represent the combined effect of a number of mismatches, it must be assumed that each of these are quite small so that significant traps of stored energy, do not exist, thereby making an adjustment in the loop loss parameter γ unnecessary. The accelerator structure, of course, stores considerably more energy per unit length than the feedback waveguide but this is taken into account in the accelerator attenuation parameter τ.

It will be assumed that any phase shift caused by the reflection Γ will be absorbed in the total loop phase length term ϕ. It is necessary however, that the phase of the transmitted wave be related to the phase of reflected wave by $\pm\pi/2$.[6] This is taken care of by the "j" term in the reflection scattering matrix. A positive "j" is used but a negative j will give the same results.

A schematic of the accelerator/waveguide loop is shown in Fig. 1. For this analysis the mismatch will be assumed to be located close to the output end of the accelerator. This will eliminate the need to separate γ into two parts. The location does not affect the final result however.

The complete set of loop equations are now

$$b_1 = \left(\frac{g}{1+g}\right)^{1/2} a_2 + j\left(\frac{1}{1+g}\right)^{1/2} a_4 \tag{21}$$

$$b_2 = \left(\frac{g}{1+g}\right)^{1/2} a_1 + j\left(\frac{1}{1+g}\right)^{1/2} a_3 \tag{22}$$

$$b_3 = \left(\frac{g}{1+g}\right)^{1/2} a_4 + j\left(\frac{1}{1+g}\right)^{1/2} a_2 \tag{23}$$

$$b_4 = \left(\frac{g}{1+g}\right)^{1/2} a_3 + j\left(\frac{1}{1+g}\right)^{1/2} a_1 \tag{24}$$

$$a_1 = V_s \tag{25}$$

$$a_2 = 0 \tag{26}$$

$$a_3 = b_4(1-\Gamma^2)^{1/2} e^{-(\tau+\gamma+j\phi)} - j(1-\Gamma^2)^{1/2} e^{-(\gamma+j\psi)} \frac{(1-e^{-\tau})}{(2\tau)^{1/2}} i_n a_1 + j\Gamma b_3 e^{-2(\gamma+j\phi_2)} \tag{27}$$

$$a_4 = b_3(1-\Gamma^2)^{1/2} e^{-(\gamma+\tau+j\phi)} + j\Gamma e^{-2(\tau+j\phi_1)} \left[b_4 + j e^{-(\gamma+j\psi)} \frac{(1-e^{-\tau})}{(2\tau)^{1/2}} i_n a_1 \right] \tag{28}$$

where ϕ_1 is the electrical length from arm 4 of the bridge to the mismatch and ϕ_2 is the electrical length from the mismatch to arm 3 of the bridge.

The loop Eqs. (21) through (24) are the same as those for the ideal reflectionless accelerator/loop network. Equations (27) and (28) must now replace Eqs. (15) and (16) to provide a complete set of loop equations which completely describe all the steady-state waves in the non-ideal system with reflections in the loop.

Effect of Reflection on Beam Energy

The wave of most interest of course is the steady-state accelerating voltage wave b_4. Solving the new set of loop equations one obtains

$$\frac{V_0}{V_s} = \frac{b_4}{a_1} = j \frac{\left[(1+g)^{1/2} - g^{1/2}(1-\Gamma^2)^{1/2} e^{-(\tau+\gamma+j\phi)}\right]\left[1 - g^{1/2} e^{-(\gamma+j\psi)} \frac{(1-e^{-\tau})}{(2\tau)^{1/2}} i_n\right]}{1+g+ge^{-2(\tau+\gamma+j\phi)} - 2g^{1/2}(1+g)^{1/2}(1-\Gamma^2)^{1/2} e^{-(\tau+\gamma+j\phi)}} . \quad (29)$$

It is too difficult to tell by inspection how this normalized wave varies with the magnitude of the effective net reflection coefficient Γ. If $\psi = 0$, $\phi = 0$, $\Gamma \ll 1$ and $(\tau + \gamma) \ll g^{-1}$, Eq. (29) simplifies approximately to

$$\frac{V_0}{V_s} \approx \frac{2g^{1/2}}{1 + (2g\Gamma)^2} \left[1 - \left(\frac{i_n^2 g \tau}{2}\right)\right]^{1/2} . \quad (30)$$

From Eq. (30) we see that the accelerating wave is affected even by very small values of Γ. A net voltage reflection coefficient of $\Gamma = (2g)^{-1} \approx 1 \times 10^{-4}$ will cause a 50% reduction in electron beam energy. Equation (29) reduces to Eq. (19) for $\Gamma = 0$. A plot of the normalized accelerating voltage wave versus loop reflection coefficient Γ is shown in Fig. 2.

For a very small net reflection we can simplify further by expressing incremental change in beam energy in terms of Γ. For $\Gamma \ll (2g)^{-1}$ the incremental change in beam energy is given by

$$\frac{\Delta V}{V} \approx -(2g\Gamma)^2 . \quad (31)$$

In simplifying Eq. (29) it was assumed that ψ, the electron bunch phase and ϕ, the phase length around the loop were 0 and n 2π respectively. It can be shown that Eq. (29) can exhibit a double peak resonance as ϕ is varied for a certain range of Γ's. The separation between these peaks becomes greater as Γ becomes larger. This characteristic will be discussed in more detail in the section of this paper dealing with combined mismatch and phase perturbations.

The Backward Wave

We have seen the effect of a small mismatch within the loop in the forward wave which is the accelerating voltage wave. The backward wave that is generated can also build up to a very high level. Solving Eqs. (21) through (28)

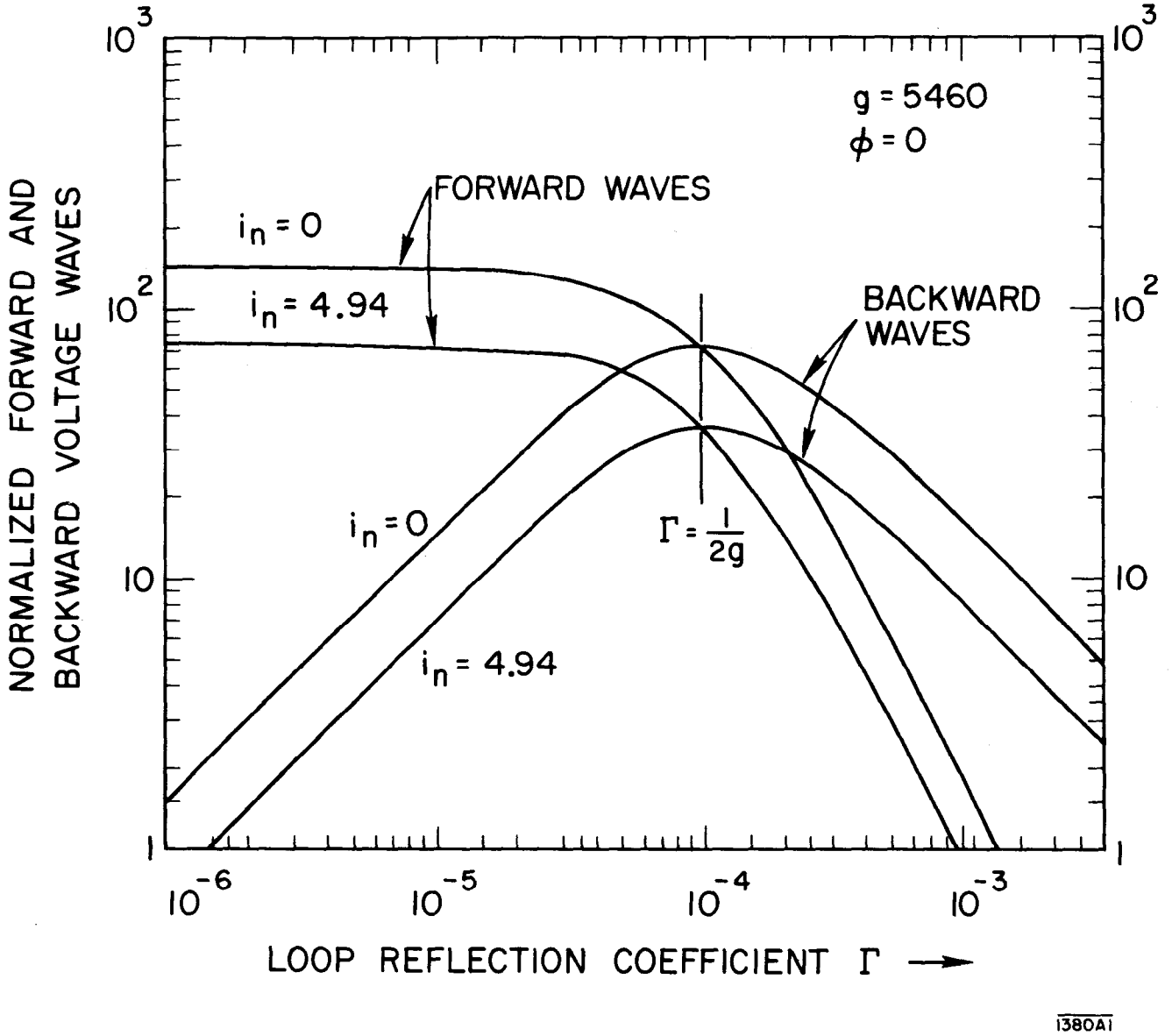

Fig. 2

The steady state forward (accelerating) and backward waves vs magnitude of a single discreetly located discontinuity within the accelerator loop. These waves are normalized to the wave incident upon arm 1 of the bridge coupler.

for a_4/a_1 gives the normalized reverse wave in the accelerator loop. This is

$$\frac{V_{0(\text{reverse})}}{V_s} = \frac{(1+g)^{1/2}\Gamma\left[1 - g^{1/2}e^{-(\gamma+j\psi)} - \frac{(1-e^{-\tau})}{(2\tau)^{1/2}} i_n\right]}{1+g+ge^{-2(\tau+\gamma+j\phi)} - 2g^{1/2}(1+g)^{1/2}(1-\Gamma^2)^{1/2}e^{-(\tau+\gamma+j\phi)}} . \quad (32)$$

This expression has the form of a resonance curve and is plotted as a function of Γ along with the accelerating wave in Fig. 2. It was noted that the accelerating wave has dropped in half for $\Gamma \approx (2g)^{-1}$ from the $\Gamma = 0$ value. At $\Gamma \approx (2g)^{-1}$ the reverse wave has reached a maximum where it is equal to the accelerating (forward) wave. This results in an infinite standing wave ratio field configuration within the accelerator loop. The backward wave, as mentioned previously, does not undergo any net energy exchange with the electron beam.

For $\Gamma \ll 1$ Eq. (32) can be expressed approximately as

$$\frac{V_{0(\text{reverse})}}{V_s} \approx \frac{4g^{3/2}\Gamma}{1+(2g\Gamma)^2}\left[1 - \left(\frac{i_n^2\, g\tau}{2}\right)^{1/2}\right] . \quad (33)$$

The reverse wave is greater than the accelerating (forward) wave for all values of $\Gamma > (2g)^{-1}$. $(2g)^{-1}$ is approximately 1×10^{-4}.

It should be mentioned at this point that if the directivity of a monitor coupler placed in the loop is poor, the signal observed will be some combination of the forward and reverse waves (the forward wave contribution being larger). This signal will always become greater as Γ becomes smaller, hence stringent monitor coupler directivity is not a requirement for tuning out a reflection Γ. This can be seen from Fig. 2.

Ratio of Backward to Forward Wave

Also of interest is the ratio of the two waves in the accelerator loop. Solution of Eqs. (21) through (28) for a_4/b_4 gives the ratio of the backward wave to the forward wave as

$$\frac{V_{0(\text{reverse})}}{V_{0(\text{forward})}} = \frac{(1+g)^{1/2}\Gamma}{(1+g)^{1/2} - g^{1/2}(1-\Gamma^2)^{1/2}e^{-(\tau+\gamma+j\phi)}} \quad (34)$$

and is independent of electron beam current.

This expression also has the form of a resonance curve, but can be misleading since the magnitude of the backward wave is indeed quite small when this ratio reaches its maximum value. The plot of this ratio as a function of Γ is shown in Fig. 3. It is noted that this ratio can exceed unity by a considerable amount. Therefore, even though the initial wave is coupled in the forward direction, the resulting steady state backward wave may exceed the forward wave. Equation (34) can be simplified considerably for $\Gamma \ll 1$ and $g \ll (\tau + \gamma)^{-1}$ to

$$\frac{V_{0(\text{reverse})}}{V_{0(\text{forward})}} \approx \frac{2g\Gamma}{1 + g\Gamma^2} \quad . \tag{35}$$

Some may prefer to call this ratio the steady-state effective loop reflection coefficient. It is interesting to note that this ratio reaches a maximum value of

$$\frac{V_{0(\text{reverse})}}{V_{0(\text{forward})}} \approx g^{1/2} \tag{36}$$

at a net voltage reflection coefficient of

$$\Gamma \approx g^{-1/2} \quad . \tag{37}$$

Equation (34) is valid for all values of Γ. For $\Gamma = 1$ this ratio again becomes unity as it did at $\Gamma \approx (2g)^{-1}$.

The above, however, assumes that $\phi = 0 (\text{or } 2n\pi)$. It is interesting to note from Eq. (32) we can solve for the accelerating wave for $\Gamma = 1$ which is

$$\frac{V_0}{V_s} = \frac{(1+g)^{1/2}\left[1 - g^{1/2} e^{-(\gamma + j\psi)} \dfrac{1 - e^{-\tau}}{(2\tau)^{1/2}} i_n\right]}{1 + g + g e^{-2(\tau + \gamma + j\phi)}} \tag{38}$$

and is very small for $\phi = 0$. However, by changing the phase length of the loop by $\phi = \pm \pi/2$, Eq. (38) becomes

$$\frac{V_0}{V_s} = \frac{(1+g)^{1/2}\left[1 - g^{1/2} e^{-(\gamma + j\psi)} \dfrac{1 - e^{-\tau}}{(2\tau)^{1/2}} i_n\right]}{1 + g\left[1 - e^{-2(\tau + \gamma)}\right]} \tag{39}$$

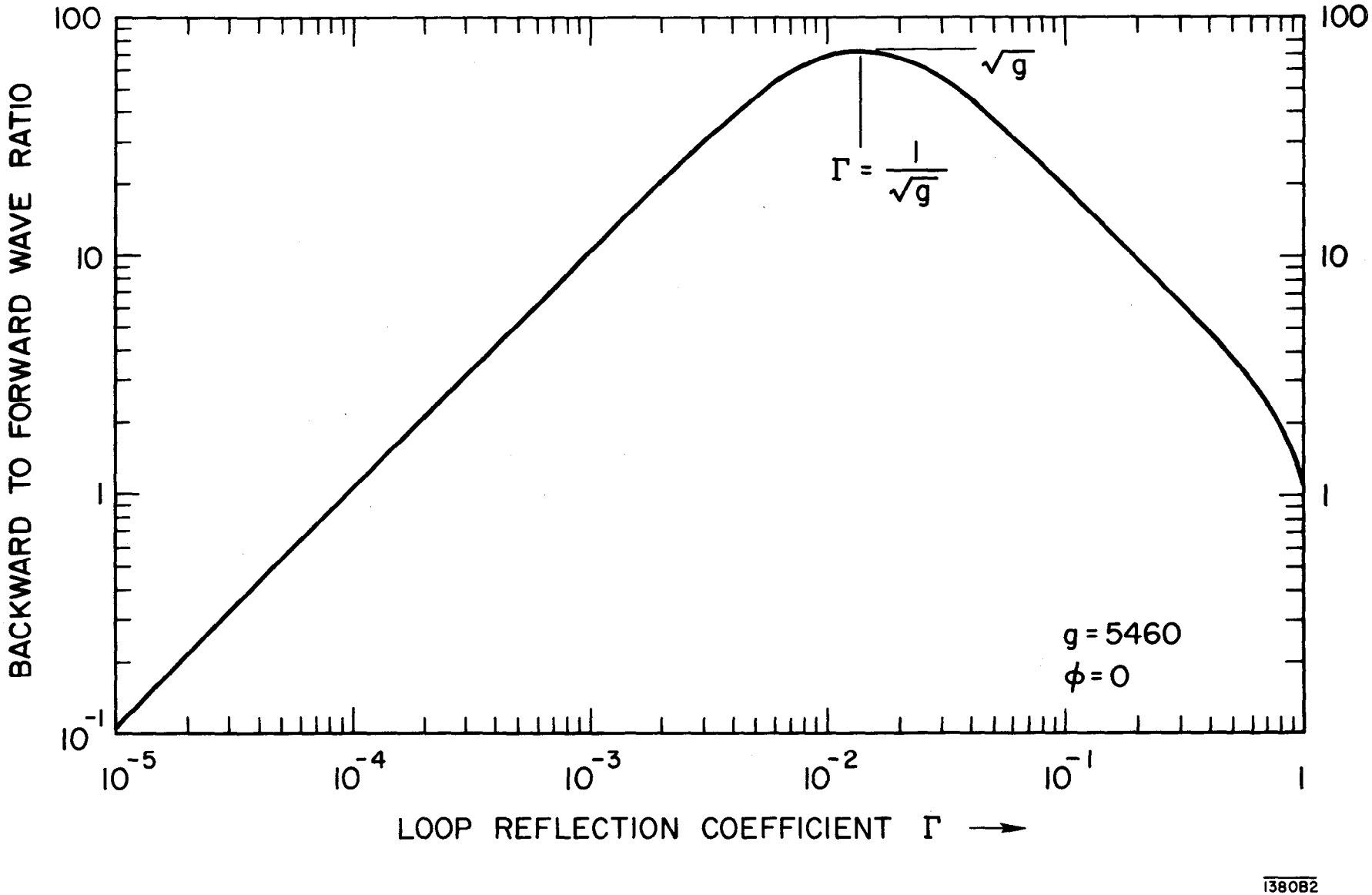

Fig. 3

The steady state ratio of the backward wave to the forward wave as a function of a reflection within the loop. This ratio is independent of beam current and exceeds unity for all values of $\Gamma > 1/2\,g$.

and for $g \ll (\tau + \gamma)^{-1}$ becomes

$$\frac{V_0}{V_s} \approx g^{1/2}\left[1 - \left(\frac{i_n^2 g\tau}{2}\right)^{1/2}\right] \tag{40}$$

giving a standing wave accelerator with one-half the design energy at the design current and equal to the design energy at zero electron beam current.

Effect of Reflection on Input Impedance to the Bridge Coupler

The high backward wave which may build up in the accelerator/waveguide loop will also make its presence known at the waveguide input to the bridge coupler. This input reflection coefficient which can be called Γ_g is given exactly by

$$\Gamma_g = \frac{b_1}{a_1} = \frac{\Gamma\left[1 - g^{1/2} e^{-(\gamma + j\psi)} \frac{1 - e^{-\tau}}{(2\tau)^{1/2}} i_n\right]}{1 + g + g e^{-2(\tau + \gamma + j\phi)} - 2g^{1/2}(1+g)^{1/2}(1-\Gamma^2)^{1/2} e^{-(\tau + \gamma + j\phi)}} \cdot \tag{41}$$

This input reflection coefficient exhibits a resonance as shown in the plot in Fig. 4. The value of Γ_g depends on the electron beam current and phase. The plot shows Γ_g as a function of Γ for zero electron beam current and for the design value of electron beam current. It is seen that the input reflection coefficient to the bridge becomes unity when the loop reflection coefficient $\Gamma = (2g)^{-1}$. For the specified value of $g = 0.546 \times 10^4$ there is virtually a short circuit at the input to the bridge for $\Gamma \approx (2g)^{-1} \approx 1 \times 10^{-4}$, if the electron beam current is zero. At the design beam current the input reflection coefficient is 0.5 at this resonance.

If the proposed scheme where a single klystron feeds two accelerator/loop systems is used, the reflection coefficient seen by the klystron will be down by a factor of two from Γ_g at the bridge providing the other accelerator/waveguide system is well matched. However, it is more likely that both accelerator loops will contribute to a mismatch at the klystron. The reflection coefficient seen at the klystron is given by

$$\Gamma_k = \frac{\Gamma_{g1} + \Gamma_{g2} e^{-j\theta}}{2} \tag{42}$$

where Γ_k is the reflection coefficient seen by the klystron and Γ_{g1} and Γ_{g2} are the respective input reflection coefficients at the respective bridges for each of the two accelerator loops. θ is the phase angle between the two waves. Γ_k

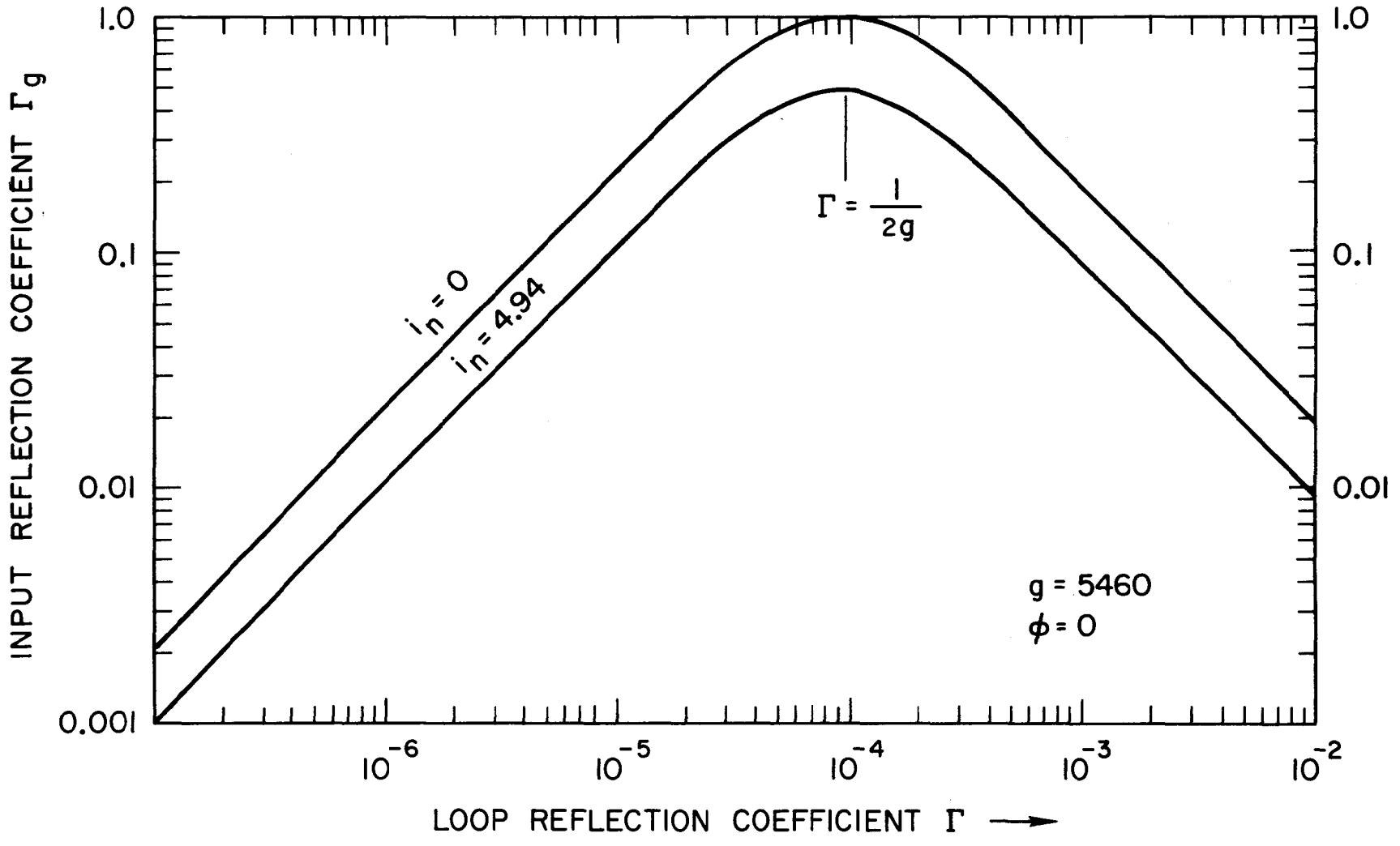

Fig. 4

138083

The steady state reflection coefficient looking into arm 1 of the bridge coupler. This is a special case for $\phi = 0$ or $2n\pi$.

can be as high as unity at zero beam current and as high as 0.5 at the design beam current.

Effect of Reflection in Dummy Load on Beam Energy

If the rf dummy load that is connected to arm 2 of the bridge coupler is not perfectly reflectionless, it is possible for a backward wave to build up in the accelerator loop. This wave is small compared to the forward wave and does not build up to nearly the extent of the backward wave caused by an equivalent reflection within the loop. A steady-state backward wave will be present only when there is a steady-state wave traveling towards the load. At the design beam current there is no power to the load and the mismatch has no effect once steady-state conditions are established.

Referring to Eqs. (9) through (16) we can substitute in place of Eq. (14)

$$a_2 = \Gamma_L b_2 \tag{43}$$

where Γ_L is the reflection coefficient for the dummy load. Solving Eqs. (9) through (16) with Eq. (43) substituted for (14) we obtain the normalized reverse wave due to a mismatch in the dummy load. This is

$$\frac{V_{0(\text{reverse})}}{V_s} = \Gamma_L \left\{ \frac{g^{1/2} - (1+g)^{1/2} e^{-(\tau+\gamma+j\phi)} + e^{-(\gamma+j\psi)} \frac{1-e^{-\tau}}{(2\tau)^{1/2}} i_n}{\left[(1+g)^{1/2} - g^{1/2} e^{-(\tau+\gamma+j\phi)}\right]^2} \right\}. \tag{44}$$

When $i_n \approx (2g\tau)^{-1/2}$, then Eq. (44) goes approximately to zero in the steady-state condition for all values of Γ_L. Where $g \ll (\tau+\gamma)^{-1}$ Eq. (44) reduces approximately to

$$\frac{V_{0(\text{reverse})}}{V_s} \approx 2g^{1/2} \Gamma_L \left[1 - (2g\tau)^{1/2} i_n\right] \tag{45}$$

The normalized backward wave is plotted as a function of normalized beam current, i_n, for various values of load reflection coefficient Γ_L in Fig. 5.

Also of interest is the ratio of the backward wave to the forward wave in the accelerator loop in the presence of a load mismatch. This is obtained by dividing Eq. (14) by Eq. (19) giving

$$\frac{V_{0(\text{reverse})}}{V_0} = \Gamma_L \left\{ \frac{g^{1/2} - (1+g)^{1/2} e^{-(\tau+\gamma+j\phi)} + e^{-(\gamma+j\psi)} \frac{1-e^{-\tau}}{(2\tau)^{1/2}} i_n}{\left[(1+g)^{1/2} - g^{1/2} e^{-(\tau+\gamma+j\phi)}\right]\left[1 - g^{1/2} e^{-(\gamma+j\psi)} \frac{1-e^{-\tau}}{(2\tau)^{1/2}} i_n\right]} \right\} \tag{46}$$

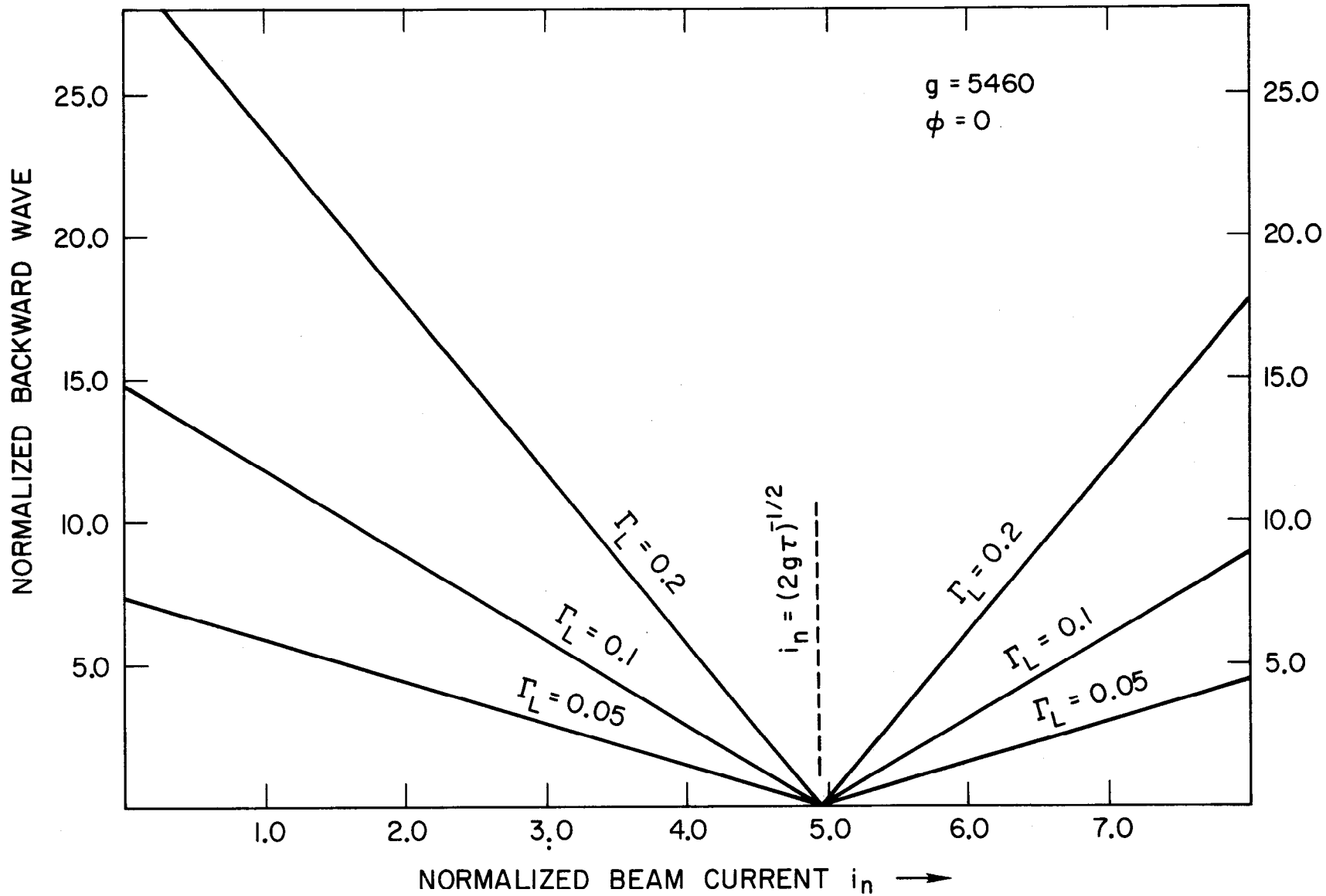

Fig. 5

1380B4

A steady state backward wave can also exist when the dummy load is not perfectly matched but only if the beam current is not equal to the design current. The normalized backward wave is shown vs normalized beam current for various dummy load reflection coefficients.

This ratio is zero when the electron beam current is equal to the design current since no power is going to the dummy load. The ratio is infinite when the electron beam current is equal to twice the design current since the forward accelerating wave is exactly canceled by the wave induced by the beam. The ratio is shown in Fig. 6. Using the aforementioned assumptions, Eq. (46) reduces approximately to

$$\frac{V_{0(\text{reverse})}}{V_0} \approx 2g\Gamma_L \left[\frac{1 - (2g\tau)^{1/2} i_n}{2 - (2g\tau)^{1/2} i_n} \right] . \tag{47}$$

Equation (47) gives a very good approximation for Eq. (46) for all values of Γ_L.

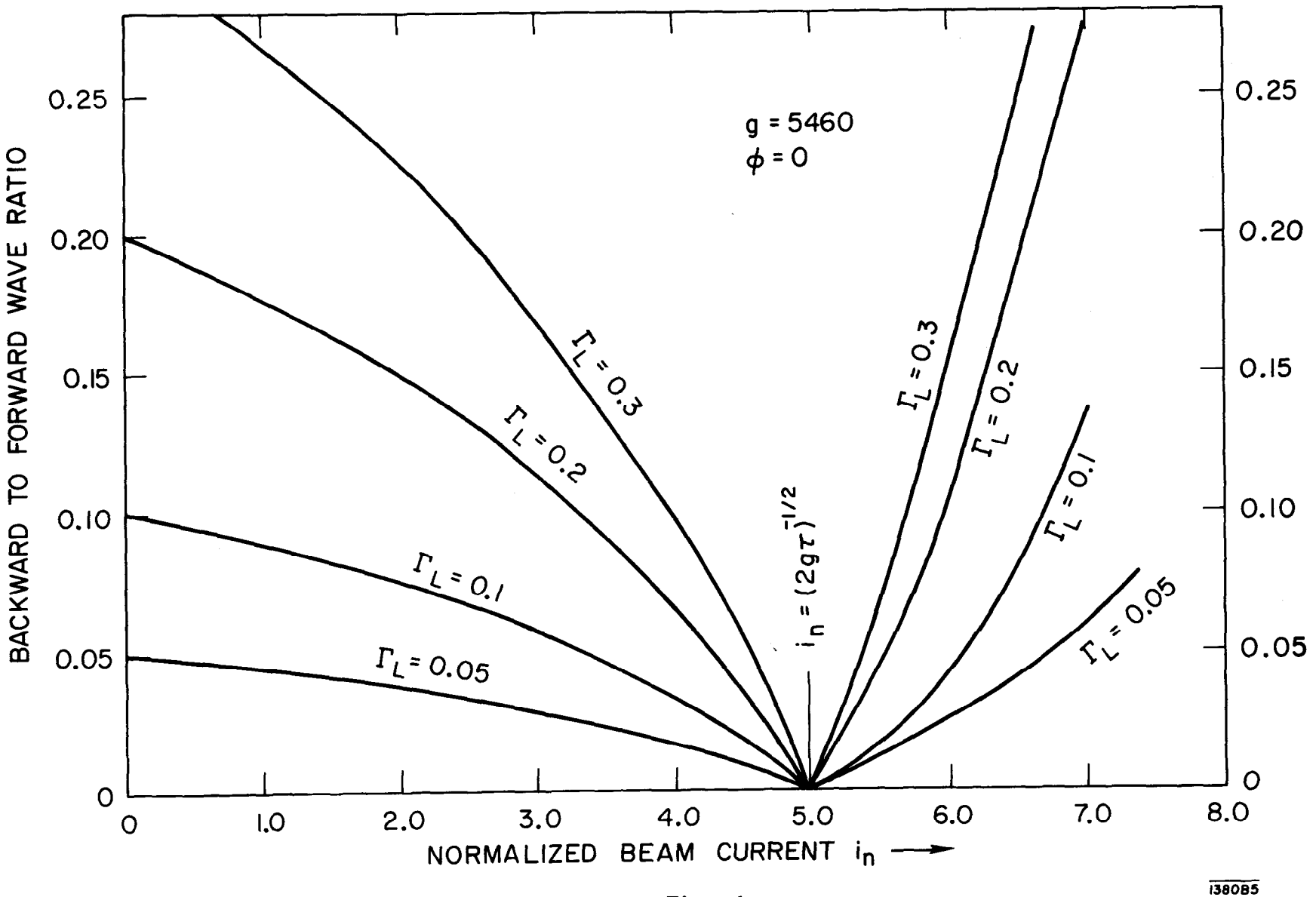

Fig. 6

The steady state backward to forward wave ratio vs normalized beam current for various dummy load reflection coefficients (see Fig. 5 caption). This ratio becomes infinite at twice the design current.

Part II – Phase Perturbations

General

The previous discussion dealt with the effect of mismatches within the accelerator loop and in the dummy load on the waves of interest in the system. The exact expressions took into account the phase length through the accelerator and around through the feedback loop. The curves that were plotted and the simplified approximations, however, were based on the assumption that ϕ, the electrical length of the path around the loop was an exact multiple of 2π. It was also assumed that the electron beam bunches were in phase with the accelerating wave.

The exact expressions for the various waves were given in complex form (i.e., the expressions contain both a real and an imaginary part except when both ϕ and ψ are equal to $2n\pi$ or 0). In order to see more clearly the phase relationship between the electron beam and the resultant rf wave, for various phasing imperfections, the expressions can be expanded and converted to polar form. Three cases will be examined. These are: 1) Where the loop length is not an integral number of wavelengths (i.e., $\phi \neq 2n\pi$); 2) the electron bunches are not in phase with the impressed rf wave (i.e. $\psi \neq 0$); and 3) both the beam and loop are misphased (i.e., $\psi \neq 0$ and $\phi \neq 2n\pi$). The polar expressions will be developed first, then drawn in phasor form. It will be assumed in this section that the accelerator loop is perfectly reflectionless.

Equation (19) may be separated into two parts: the steady state wave due to the rf driving source alone and the steady state wave induced by the electron beam. From Eq. (19) we can obtain the normalized steady state wave due to the impressed rf. This is given in polar form by

$$\left.\frac{V_0}{V_s}\right|_{rf} = \frac{1 \angle \beta}{\left[1+g+ge^{-2(\tau+\gamma)} - 2g^{1/2}(1+g)^{1/2}e^{-(\tau+\gamma)}\cos\phi\right]^{1/2}} \tag{48}$$

where

$$\beta = -\arctan\left[\frac{g^{1/2}e^{-(\tau+\gamma)}\sin\phi}{(1+g)^{1/2} - g^{1/2}e^{-(\tau+\gamma)}\cos\phi}\right] \tag{49}$$

and ϕ can now be considered the phase deviation from $2n\pi$ around the loop.

For small values of ϕ Eq. (48) reduces approximately to

$$\left.\frac{\overline{V}_0}{\overline{V}_s}\right|_{rf} \approx \frac{2g^{1/2} \angle -2g\phi}{1+2(g\phi)^2} \tag{50}$$

and Eq. (49) to

$$\beta \approx -2g\phi \tag{51}$$

The angle β is a vector direction with respect to the impressed rf vector before buildup which has zero angle.

From Eq. (19) the normalized steady state wave induced by the bunched electron beam is obtained and is given in polar form by

$$\left.\frac{\overline{V}_0}{\overline{V}_s}\right|_{\text{Induced}} = -\frac{g^{1/2}e^{-\gamma}\,\frac{1-e^{-\tau}}{(2\tau)^{1/2}}\,i_n \angle \psi+\beta}{\left[1+g+ge^{-2(\tau+\gamma)} - 2g^{1/2}(1+g)^{1/2}e^{-(\tau+\gamma)}\cos\phi\right]^{1/2}} \tag{52}$$

For small values of ϕ Eq. (52) reduces approximately to

$$\left.\frac{\overline{V}_0}{\overline{V}_s}\right|_{\text{Induced}} \approx -\frac{(2\tau\, g^2)^{1/2} i_n}{1+2(g\phi)^2} \angle \psi - 2g\phi \tag{53}$$

At the design beam current, $i_n \approx (2g\tau)^{-1/2}$, the steady state beam induced vector expressed by Eq. (53) is one-half the steady state rf vector expressed by Eq. (48).

The vector addition of Eqs. (48) and (52) gives the resultant of the two waves as

$$\left.\frac{\overline{V}_0}{\overline{V}_s}\right|_{\text{Resultant}} = \left[\frac{1+ge^{-2\gamma\frac{(1-e^{-\tau})}{2\tau}}\,i_n^2 - 2g^{1/2}e^{-\gamma\frac{(1-e^{-\tau})}{(2\tau)^{1/2}}}\,i_n\cos\psi}{1+g+ge^{-2(\tau+\gamma)} - 2g^{1/2}(1+g)^{1/2}e^{-(\tau+\gamma)}\cos\phi}\right]^{1/2} \angle \Upsilon \tag{54}$$

where

$$\Upsilon = \arctan\left[\frac{\sin\beta - g^{1/2}e^{-\gamma}\frac{(1-e^{-\tau})}{(2\tau)^{1/2}}\,i_n\sin(\beta+\psi)}{\cos\beta - g^{1/2}e^{-\gamma}\frac{(1-e^{-\tau})}{(2\tau)^{1/2}}\,i_n\cos(\beta+\psi)}\right] \tag{55}$$

Simplifying as before

$$\left.\frac{\overline{V}_0}{V_s}\right|_{\text{Resultant}} \approx 2g^{1/2}\,\frac{\left[1-(2g\tau)^{1/2}i_n\left(1-\frac{\psi^2}{2}\right)+1/2g\tau\, i_n^2\right]^{1/2}}{1+2(g\phi)^2}\;\angle\Upsilon \qquad (56)$$

The above expressions, Eqs. (48) through (56) completely describe the various combinations of steady state electron bunch phase and loop phase perturbations. The three cases mentioned earlier are illustrated in the vector diagrams in Figs. 7 through 9.

Case with Loop Phase Error Only ($\phi \neq 2n\pi$, $\psi = 0$)

The accelerating wave buildup is shown in Fig. 7 for the case where there is a phase error in the length of the accelerator and feedback loop. In this case ϕ is the deviation in loop length from $2n\pi$. The small arrows in the first quadrant of Fig. 7 represent the first three transits of the impressed rf vector, $V_s/(1+g)^{1/2}$. V_{rf} is the steady state rf wave due to the driving source after an infinite number of trips around the loop. V_{rf} would normally have a length of approximately $2g^{1/2}$ if there were no loop phase error. The length of V_{rf} with a loop phase error ϕ is given exactly by Eq. (48) and approximately by Eq. (50).

The buildup of the wave induced by the electron beam is the same as the buildup of the klystron wave except that it will normally (if $\psi = 0$) by 180 degrees out of phase with the driven wave. The resultant wave will be the vector addition of V_{rf} and $V_{induced}$ which is simply the difference in their magnitudes for $\psi = 0$. Since ψ is defined as the phase angle between the electron bunches and the impressed rf wave before buildup, there will be a phase error between the electron bunches and the steady state resultant wave as shown in Fig. 7. The bunches will be off of the crest of the steady state accelerating wave (the vector sum of the driven wave and the induced wave) by an angle β defined by Eq. (49). Adding Eqs. (50) and (53) gives

$$\left.\frac{\overline{V}_0}{V_s}\right|_{\text{Resultant}} \approx \frac{2g^{1/2}}{1+2(g\phi)^2}\left[1-\left(\frac{\tau g}{2}\right)^{1/2}i_n\right] \qquad (57)$$

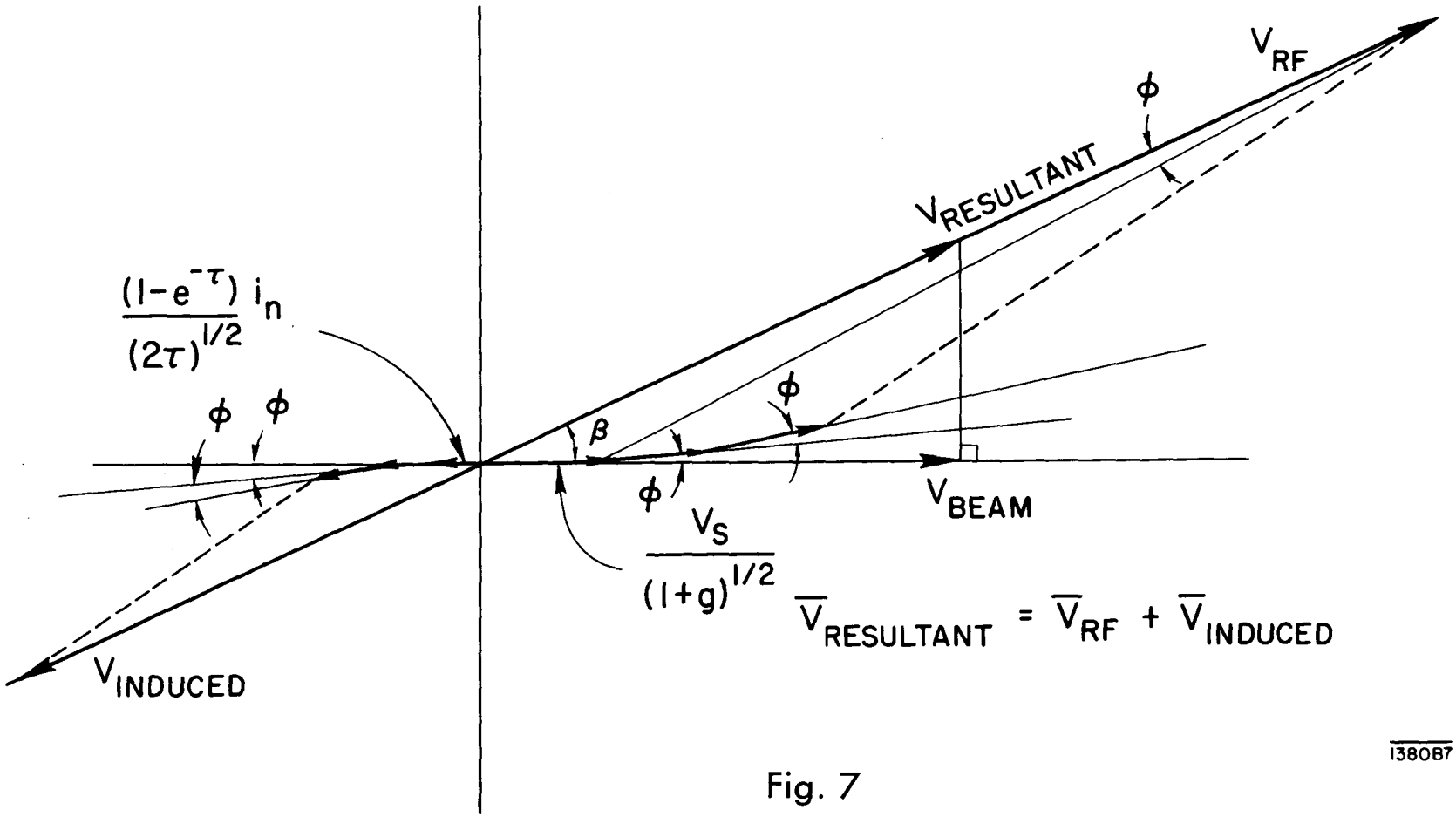

138087

Fig. 7

The first three trips around the loop for both the driven and induced waves are shown to illustrate the buildup when there is a phase error ϕ in the length of the loop.

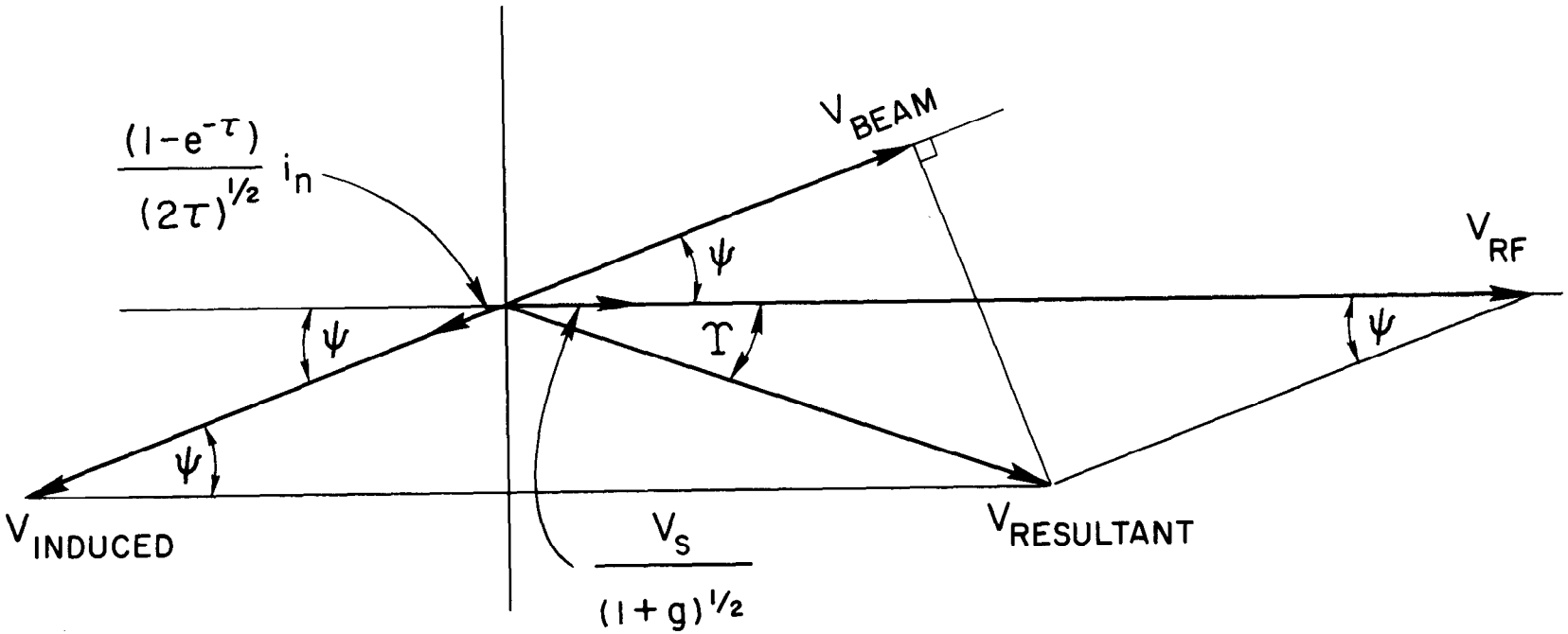

$$\bar{V}_{RESULTANT} = \bar{V}_{RF} + \bar{V}_{INDUCED}$$

$$\left| V_{BEAM} \right| = \left| V_{RESULTANT} \right| \cos(\Upsilon + \Psi)$$

1380A8

Fig. 8

A phase error ψ between the beam and the accelerating field exists. The resultant field makes an angle Υ with the driven rf wave and an angle $(\Upsilon+\psi)$ with the electron beam.

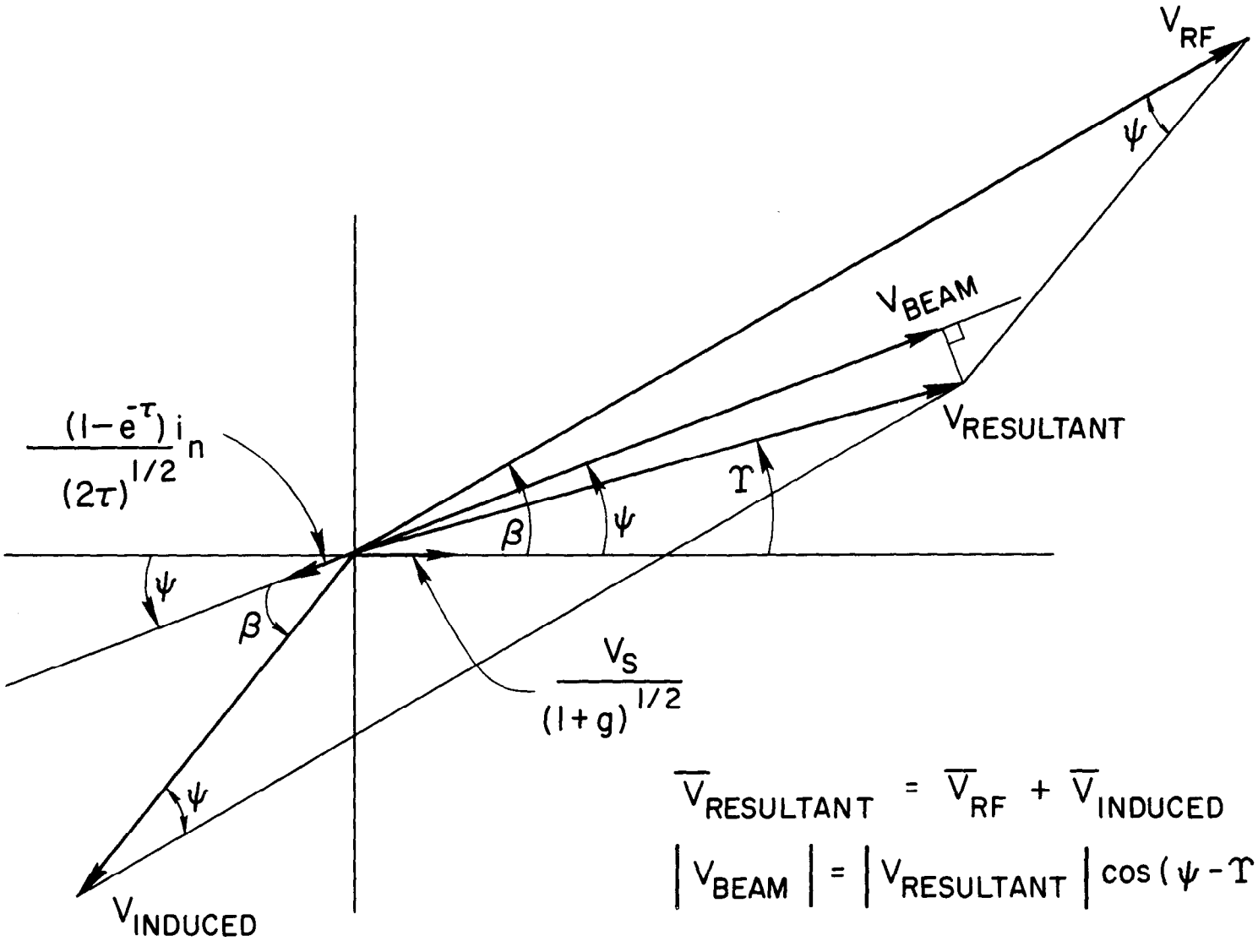

1380A6

Fig. 9

Both a beam phase error ψ relative to the impressed rf and a loop phase error ϕ exist. The electron bunches will not be in phase with $V_{resultant}$ except for the special case where $\psi = \Upsilon$. In the case shown, the beam phase error tends to compensate for the loop phase error.

for $\psi = 0$. The effective part of the resultant wave acting upon the beam is found by multiplying Eq. (57) by cos $2g\phi$ giving

$$\left.\frac{V_0}{V_s}\right|_{Beam} \approx \frac{2g^{1/2}}{1+2(g\phi)^2}\left[1-\left(\frac{\tau g}{2}\right)^{1/2} i_n\right]\cos 2g\phi \qquad (58)$$

The fractional change in beam energy due to a loop phase error ϕ is then given by

$$\left.\frac{\delta V_0}{V_0}\right|_{Beam} \approx -(2g\phi)^2 \qquad (59)$$

Case with Phase Error Between Electron Bunches and Impressed RF Wave ($\psi \neq 0,\ \phi = 0$)

If the loop length is an exact multiple of 2π but a phase error, ψ exists between the impressed rf wave and the electron bunches the vector orientation appears as shown in Fig. 8. The steady state wave, $V_{resultant}$ now makes an angle Υ with the steady state rf component V_{rf}. Υ is defined by Eq. (55). For small values of the initial beam phase error ψ

$$\Upsilon \approx \psi \qquad (60)$$

if the electron beam current is at the design value. For smaller values of electron beam current Υ also becomes smaller.

The magnitude of the resultant for this case can be found from Eq. (54) by setting $\phi = 0$. The resultant wave will always be greater than for the "in phase" case ($\psi = 0$) but the beam energy will always be slightly lower since the electron bunches will be off of the crest by an angle ($\psi + \Upsilon$). The resultant wave, $V_{resultant}$ is expressed approximately by the numerator of Eq. (56). The effective part of the resultant wave acting upon the electron beam is given by

$$\left.\frac{V_0}{V_s}\right|_{Beam} = \left.\frac{V_0}{V_s}\right|_{Resultant} \cos(\psi+\beta)$$

$$\approx 2g^{1/2}\left[1-\left(\frac{g\tau}{2}\right)^{1/2} i_n\right]\left[1-\frac{1}{2}(\psi+\Upsilon)^2\right]\left[1+\frac{\psi^2(2g\tau)^{1/2} i_n}{4\left[1-\left(\frac{g\tau}{2}\right)^{1/2} i_n\right]^2}\right] \qquad (61)$$

At the design current and for small values of ψ, the fractional change in energy is given by

$$\left.\frac{\delta V_0}{V_0}\right|_{\text{Beam}} \approx - \psi^2 \tag{62}$$

and at negligible beam loading the fractional change in energy is given by

$$\left.\frac{\delta V_0}{V_0}\right|_{\text{Beam}} \approx - \frac{\psi^2}{2} \tag{63}$$

Case with Loop Phase Error and Beam Phase Error ($\phi \neq 0$ and $\psi \neq 0$)

Figure 9 shows the vector orientation when both a loop phase error and a beam phase error exist. It must be emphasized that the beam phase error is defined in this paper as the phase angle between the electron bunches and the impressed rf wave and not the steady state rf wave. It will be seen that it is possible to have a beam phase error with respect to the impressed wave but not the steady state wave and conversely.

In the example shown the beam phase error ψ is in such a direction that it tends to compensate for the loop phase error ϕ. If ψ had the opposite sign the beam phase error would add to the loop phase error. The magnitude of the resultant wave is given by Eq. (54). The effective part of the resultant wave acting upon the electron beam is given by

$$\left.\frac{V_0}{V_s}\right|_{\text{Beam}} = \left.\frac{V_0}{V_s}\right|_{\text{Resultant}} \cos (\psi \pm \Upsilon) \tag{64}$$

The sign in the cosine argument depends upon the direction of the phase error.

The fractional change in beam energy for this case is

$$\left.\frac{\delta V_0}{V_0}\right|_{\text{Beam}} \approx - \left[2 \psi^2 + 2(g\phi)^2 + \Upsilon^2 \pm 2\Upsilon\psi \right] \tag{65}$$

at the design current.

Part III - Combined Phase and Mismatch Perturbation

General

The double peaked resonance behavior has been described by several authors[2,4,5] in papers on traveling wave resonator theory. The same theory applies to the accelerator and feedback loop and is not affected by beam loading. The behavior is as follows: For a net reflection coefficient Γ less than a critical value there is a single maximum for the accelerating wave as either frequency or phase length of the loop is varied. This maximum occurs when $\phi = 2n\pi$ where n is an integer. As Γ is increased past the critical value the resonance separates into two peaks with a valley at $\phi = 2n\pi$. The two peaks are symmetrically located about $\phi = 2n\pi$. The greater the value of Γ, the wider the separation between peaks and the smaller the magnitude of the accelerating wave. For the sake of simplicity the curves in Figs. 2, 3 and 4 assumed that $\phi = 0$ or $2n\pi$. In the range where Γ exceeded the critical value the magnitude of the accelerating wave could be increased by an adjustment of the ϕ parameter from $2n\pi$ to one of the resonant peaks. This behavior is analogous to coupled resonant circuits where the coupling (in this case the reflection magnitude) is varied. Here the two circuits are the forward and backward wave modes in the accelerator loop.

Analysis of Double Resonance

The exact behavior of the accelerator resonance can be found from Eq. (29). Expanding, the magnitude may be expressed as

$$\frac{V_0}{V_s} =$$

$$\left[\frac{\left[1+g+g(1-\Gamma^2)e^{-2(\tau+\gamma)}-2g^{\frac{1}{2}}(1+g)^{\frac{1}{2}}(1-\Gamma^2)^{\frac{1}{2}}e^{-(\tau+\gamma)}\cos\phi\right]\left[1-2g^{\frac{1}{2}}e^{-\gamma}\frac{(1-e^{-\tau})}{(2\tau)^{1/2}}i_n+ge^{-2\gamma}\frac{(1-e^{-\tau})^2}{2\tau}i_n^{\,2}\right]}{(1+g)^2+g^2e^{-4(\tau+\gamma)}+4g(1+g)(1-\Gamma^2)e^{-2(\tau+\gamma)}-4g^{\frac{1}{2}}(1+g)^{\frac{1}{2}}(1-\Gamma^2)^{\frac{1}{2}}e^{-(\tau+\gamma)}\left(1+g+ge^{-2(\tau+\gamma)}\right)\cos\phi+2g(1+g)e^{-2(\tau+\gamma)}\cos2\phi}\right] \tag{66}$$

Differentiating Eq. (66) with respect to ϕ and setting result equal to zero one obtains

$$\phi = 2n\pi \tag{67}$$

and

$$\phi = \pm \arccos\left[\frac{1+g+g(1-\Gamma^2)e^{-2(\tau+\gamma)} - \Gamma\sqrt{(1+g)^2+g^2(1-\Gamma^2)e^{-4(\tau+\gamma)}-2g(1+g)(1-\Gamma^2)e^{-2(\tau+\gamma)}}}{2g^{1/2}(1+g)^{1/2}(1-\Gamma^2)^{1/2}e^{-(\tau+\gamma)}}\right] \quad (68)$$

The minima occur at $\phi = 2n\pi$ and the maxima occur at the values of ϕ in Eq. (68). It should be noted that for a small critical value of Γ the arc cos argument is equal to unity and is slightly greater than unity in the range between $\Gamma = 0$ and the critical value. Values of ϕ for an arc cos argument greater than unity cannot exist hence this region of Γ's do not produce a double peak but only a single peak at $\phi = 2n\pi$. The critical value of Γ could be found by setting the argument in Eq. (68) to unity and rigorously solving for Γ. The argument is complicated however and the value of Γ producing unity argument can most easily be found with a graphic solution. For $g = 5460$ and $(\tau + \gamma) \ll 1/g$ the critical value of Γ is approximately

$$\Gamma_{critical} \approx 4 \times 10^{-5} \quad (69)$$

As Γ increases through and beyond this value the single peaks flatten and then separate into two distinct peaks. The maximum at $\phi = 2n\pi$ now becomes a minimum. The ambitious calculus student may verify this by taking the second derivative of Eq. (66) with respect to ϕ and equating the result to 0 and observing the sign reversal at the critical value of Γ.

An unsuccessful attempt was made to plot Eq. (66) as a function of ϕ for several values of Γ. The precision required was far greater than that for wave gain expressed where only a single perturbation of either Γ or ϕ existed such as in Eqs. (29) and (48). Approximations up to the 5th order were also not sufficiently valid.

The following table gives the location of the peaks with respect to $\phi = 2n\pi$ but does not give the magnitude of the accelerating wave at each peak.

Γ	$\Delta\phi$ (radians)	V_0/V_0 max ($\phi = 2n\pi$)
1×10^{-6}	single peak	0.9999
1×10^{-5}	single peak	0.990
1×10^{-4}	$\pm 1.11 \times 10^{-4}$	0.50
2×10^{-4}	$\pm 2.14 \times 10^{-4}$	0.28
5×10^{-4}	$\pm 5.08 \times 10^{-4}$	0.04
1×10^{-3}	$\pm 10.04 \times 10^{-4}$	0.013

From this table it is obvious that the peaks are displaced about $\phi = 2n\pi$ by approximately

$$\Delta\phi \approx \pm \Gamma \tag{70}$$

in the region where the double resonance exists.

Effect on Input Reflection Coefficient and Backward Wave

The backward wave experiences a double peaking also but the peaks occur at slightly different values of ϕ than the forward wave.[2] The accelerating (forward) wave has a pronounced double peak before the backward wave has any evidence of a double peak.[2] The resonant peaks for the backward wave and for the input reflection coefficient occur at[2]

$$\phi = \pm \arccos \left[\frac{(1 - \Gamma^2)^{1/2} \left(1 + g + ge^{-2(\tau + \gamma)}\right)}{2g^{1/2}(1 + g)^{1/2} e^{-(\tau + \gamma)}} \right] \tag{71}$$

Again the critical value of Γ at which double peaking begins to occur can be found by setting this argument in Eq. (71) to unity and solving for Γ. This yields

$$\Gamma_{\text{critical}} = \frac{1 + g - ge^{-2(\tau+\gamma)}}{1 + g + ge^{-2(\tau+\gamma)}} \tag{72}$$

For $(\tau + \gamma) \ll 1/g$ Eq. (72) can be expressed approximately as

$$\Gamma_{\text{critical}} \approx (2g)^{-1} \tag{73}$$

It was shown in Part I in the section on the "Effect of Reflection on Input Impedance to the Bridge Coupler" that the input reflection coefficient approaches unity when $\Gamma \approx (2g)^{-1}$ for $\phi = 2n\pi$ and $i_n = 0$. It can also be shown[2] that there is a corresponding value of ϕ that will produce in input reflection close to unity for all values of Γ greater than $(2g)^{-1}$.

References

1. R. B. Neal, "Consideration of the use of feedback in a traveling wave superconducting accelerator," Report No. SLAC-PUB-437, Stanford Linear Accelerator Center, Stanford University, Stanford, California (1968).
2. S. J. Miller, "The traveling wave resonator and high power microwave testing," Microwave Journal, pp. 50-58, September (1960).
3. F. J. Tischer, "Resonance properties of ring circuits," IRE Transactions PGMTT, MTT5, 51-56 (1957).
4. K. Tomiyasu, "Effect of a mismatched ring in a traveling wave resonant circuit," Transactions PGMTT, MTT5, 267 (1957).
5. P. B. Wilson, "Effect of a perturbation in a traveling wave resonator," Report No. HEPL-TN-68-6, Stanford University, Stanford, California (1968).
6. C. G. Montgomery, R. H. Dicke, E. M. Purcell, Principles of Microwave Circuits, MIT Radiation Laboratory Series, Vol. 8 (McGraw Hill, New York 1948) p. 149.
7. L. J. Milosenic and R. Vautey, "Traveling wave resonators," IRE Transactions PGMTT, MTT6, 136-143 (1958).
8. H. Golde, "Theory and measurement of Q in resonant ring circuits," IRE Transactions PGMTT, MTT8, 560-564 (1960).
9. R. B. Neal, "Sample parameters of a two-mile superconducting accelerator," Report No. SLAC-PUB-438, Stanford Linear Accelerator Center, Stanford University, Stanford, California (1968).
10. R. Alvarez, "Phase changing devices and wall deformation in rectangular waveguide," Technical Note No. SLAC-TN-69-9, Stanford Linear Accelerator Center, Stanford University, Stanford, California (1969).